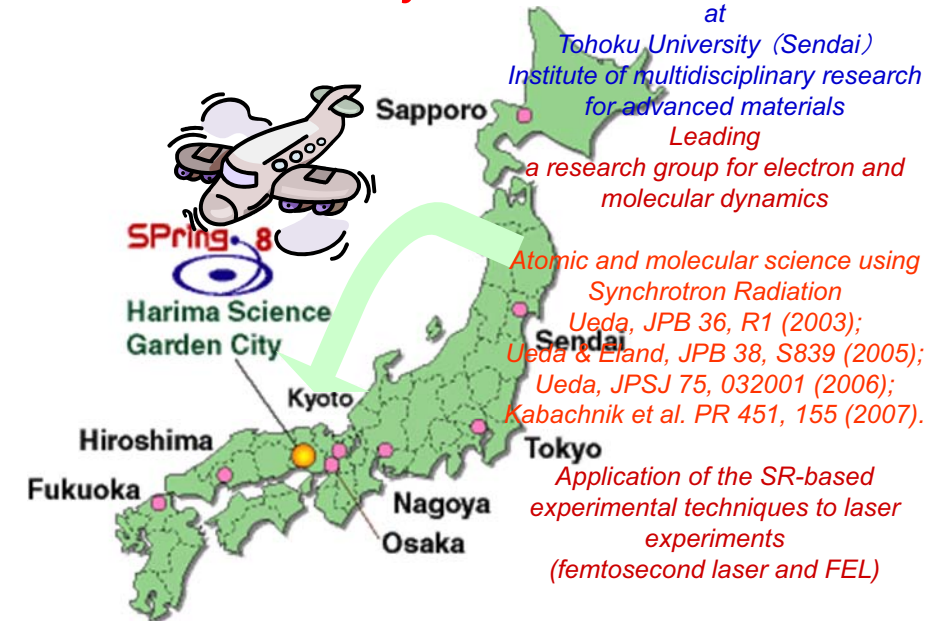




Introduction of myself



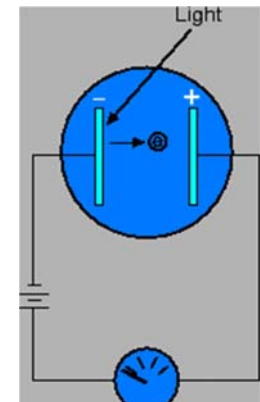
Outline

1. Introduction to quantum world
2. Atomic resonant photoemission spectroscopy
 - Introduction to the quantum interference
3. Vibrationally-resolved core-level photoelectron spectroscopy
 - Adiabatic approximation and Franck-Condon analysis
 - Young's double-slit experiments
4. Multiple-ion momentum imaging
 - Snapshots of molecular deformation within a few fs
5. Electron-ion momentum imaging
 - Molecular-frame photoelectron angular distributions
6. Interatomic Coulombic decay
7. Characteristic properties of free electron lasers
8. Atomic multi-photon processes by FEL: from EUV to X

Photoelectric effect

When matter is shined by the light, electron is emitted from the surface.

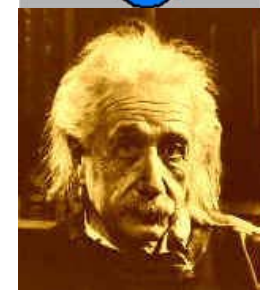
- (i) Frequency of the light needs to be larger than v_0 .
- (ii) Kinetic energy of the electron is determined by the frequency of the light.
- (iii) Number of electrons is proportional to the intensity of the light.

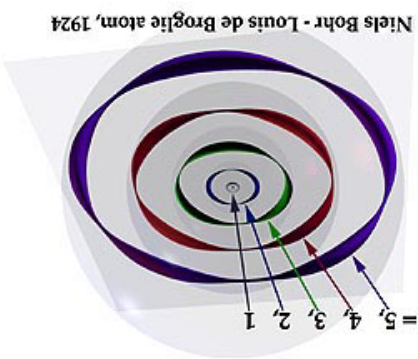


Einstein's explanation

Light at frequency of v is considered to be a group of particles (photons) and each photon has energy hv . An electron gets the energy hv when it absorbs one photon.

The electron in the matter is bound. For the electron to be emitted from the matter, the electron needs to receive the energy more than the work function W . Then the kinetic energy KE of the emitted electron can be given as $KE = hv - W$.

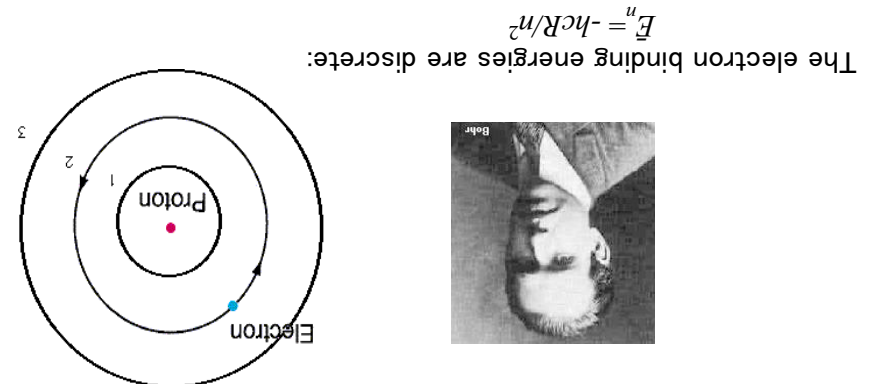




$$\alpha = \hbar/p \quad 2\pi r = n\lambda = nh/p = nh/mv$$

$$\text{Quantization: } \int_0^{2\pi} p_\phi d\phi = nh$$

De Broglie's matter wave and Bohr's model



ϕ , angle of rotation; $p_\phi = m_e r d\phi/dt$, angular momentum; r , radius; m_e , electron mass

$$\int_0^{2\pi} p_\phi d\phi = nh$$

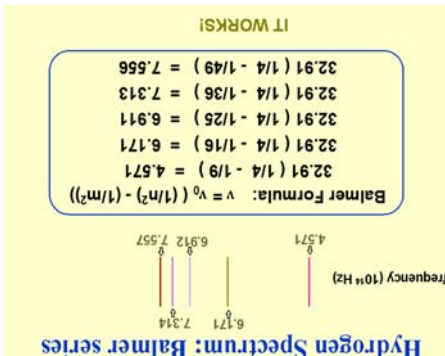
Electron orbits exist only when the classical orbits satisfy the following condition of quantization:

Bohr's atomic model

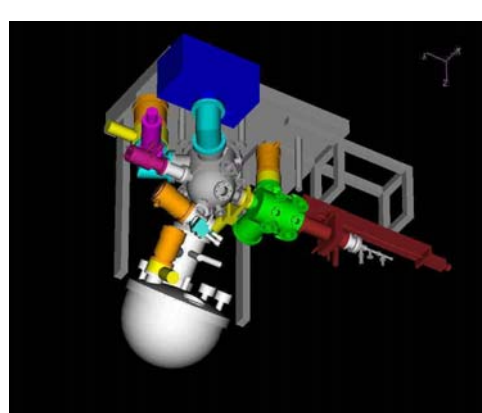
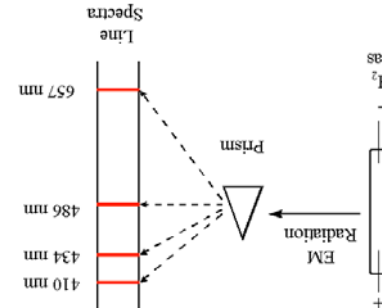
c , speed of light; λ , wavelength; R , Rydberg constant ($R = 109737.309 \text{ cm}^{-1}$)

$$\text{Rydberg formula: } \frac{1}{\lambda} = R \left(\frac{1}{n^2} - \frac{1}{m^2} \right)$$

Balmer found beautiful regularity in the H spectrum!

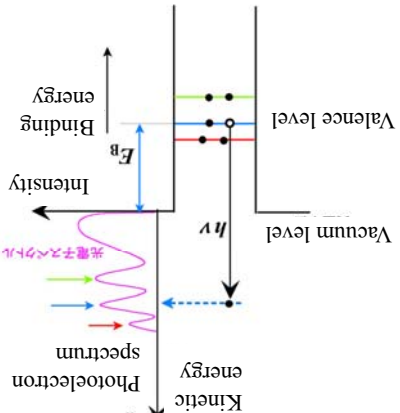


Balmer and Rydberg formulae



Precise measurements for kinetic energies of photoelectrons emitted via Einstein's photoelectric effects

Photoelectron spectroscopy (UPS, XPS)



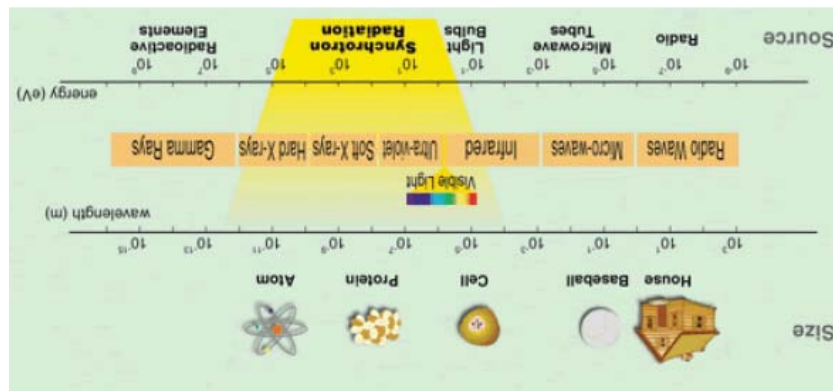
Target: single atom or molecule; size: $\sim 1 \text{ Å} (= 0.1 \text{ nm} = 10^{-10} \text{ m})$

Atomic and molecular science now



Spring-8 BL27SU

How to use synchrotron radiation to study atoms and molecules
We use monochromatic synchrotron radiation to excite atoms and molecules and to study their electronic structures as well as electron and nuclear dynamics in the excited states.
A single photon should be absorbed by a single atom or molecule first!



Schrödinger equation of H atom (in atomic units)

$$H\psi(r) = E\psi(r)$$

$$T = \frac{p^2}{2} = -\frac{1}{r^2} \frac{\partial^2}{\partial r^2}$$

momentum

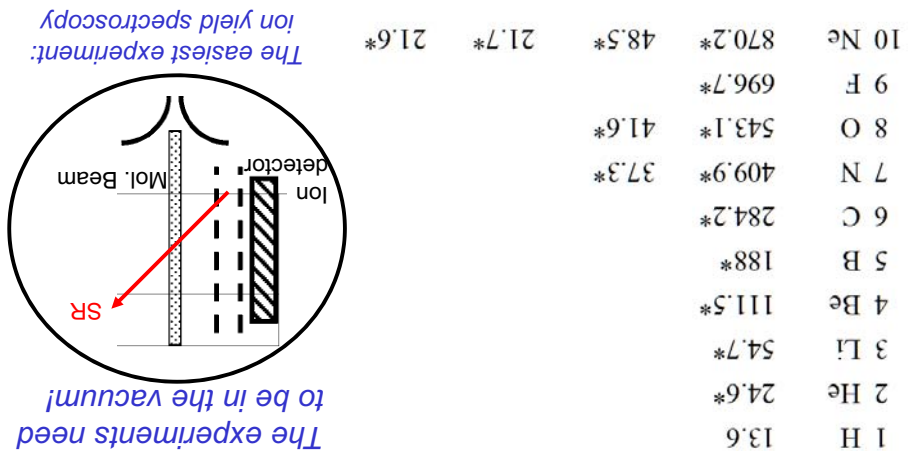
$$U(r) = -\frac{1}{r}$$

wave function

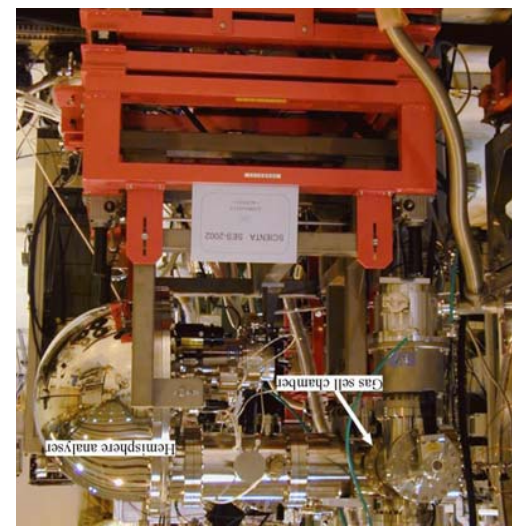
complex number (with phase!)

$$E_n = -\frac{1}{r^2}$$

Element	K 1s	L ₁ 2s	L ₂	L ₃	Vacuum ultraviolet light
1 H	13.6				2p _{1/2} 2p _{3/2}
2 He	24.6*				
3 Li	54.7*				
4 Be	111.5*				
5 B	188*				
6 C	284.2*				
7 N	409.9*	37.3*			
8 O	543.1*	41.6*			
9 F	696.7*				
10 Ne	870.2*	48.5*	21.7*	21.6*	

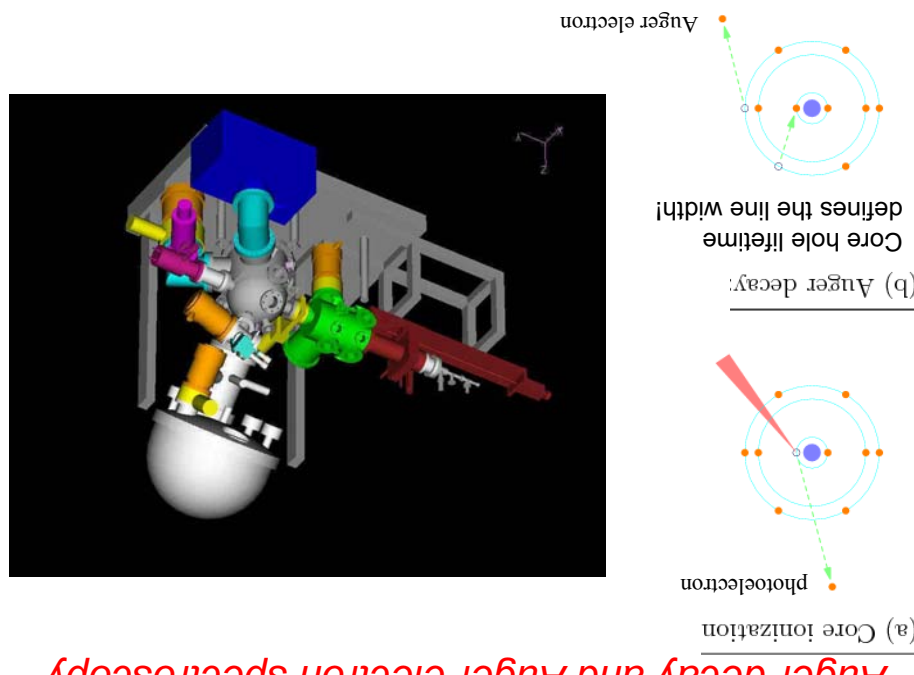


- **Electrostatic hemispherical analyzer**
- $\Delta E/E = 1/1600$
- Mean radius 200 mm
- MCP+CCD camera (66 meV at pass 100 eV)
- MCP+Delay line anode or MCP+Delay line anode
- Gas cell system
- Doppler-free molecular beam source
- Ueda et al. PRL . 90, 153005 (2003)
- Priimper et al. PRA 71, 052704, (2005).

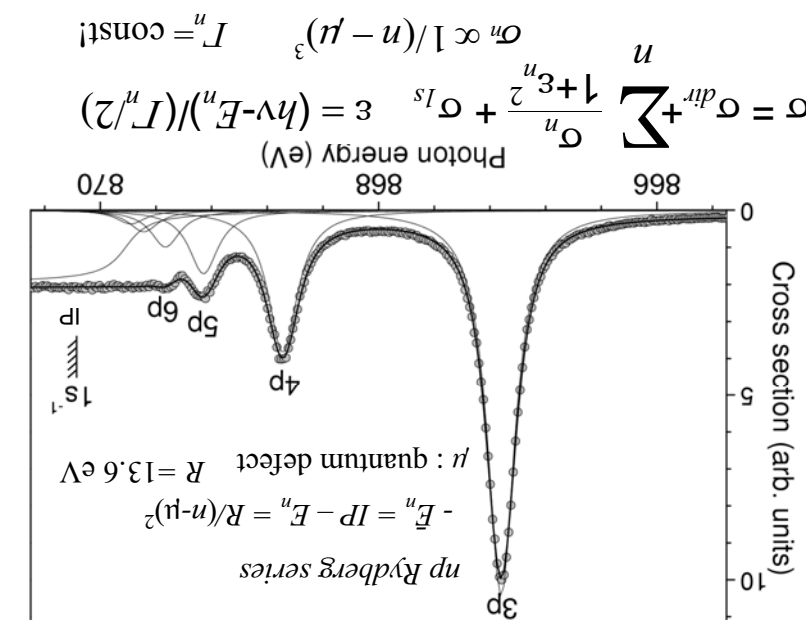


SES2002 analyzer

Angle-resolved resonant Auger spectra of Ne at



Auger decay and Auger electron spectroscopy



Born-Oppenheimer approximation

Nuclear motion is within the adiabatic potential energy surface!

$$[T^r + \epsilon^m(R)]\Phi_0^m(R) = E_0^m\Phi_0^m(R)$$

$$\Psi(R, r) = \prod_n \Phi_n^m(R)\phi_n^m(r)$$

$\epsilon^m(R)$: adiabatic potential energy

$$[H^0 - \epsilon^m(R)]\phi(R, r) = 0$$

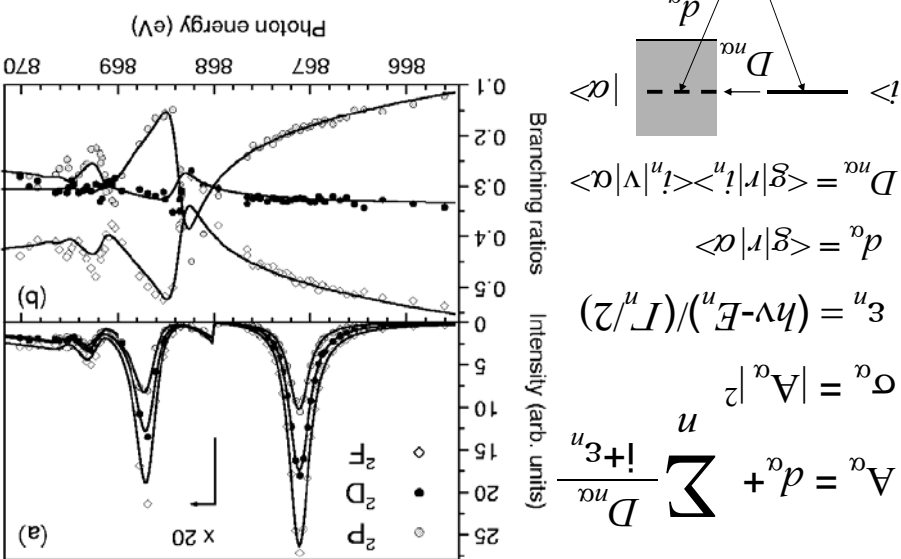
$$H = H^0 + T^r \quad H^0 = T^r + V(r, R)$$

$$T^r = -\frac{\hbar}{\mu} \sum_j M^j \frac{\partial \phi^2}{\partial r^j} \quad \text{KE of nucleus} \quad T_e = -\frac{\hbar}{\mu} \sum_j \frac{\partial^2 \phi^2}{\partial r^j \partial r^j} \quad \text{KE of electrons}$$

$$H\Psi(R, r) = E\Psi(R, r) \quad H = T^r + V(r, R)$$

Introduction of molecular world

De Fanti et al. Phys. Rev. Lett. **89**, 023006 (2002).

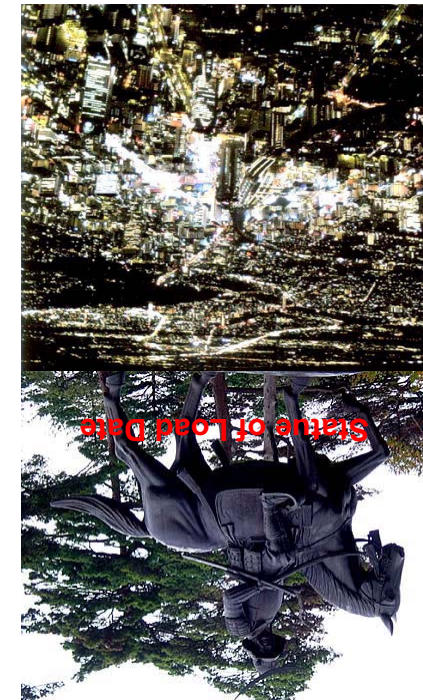
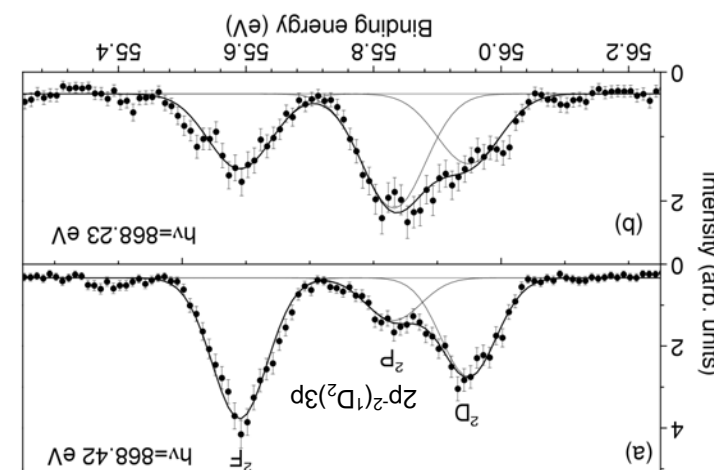


Interference effects between the two paths

$1s \rightarrow 3p$ and $1s \rightarrow 4p$ excitations

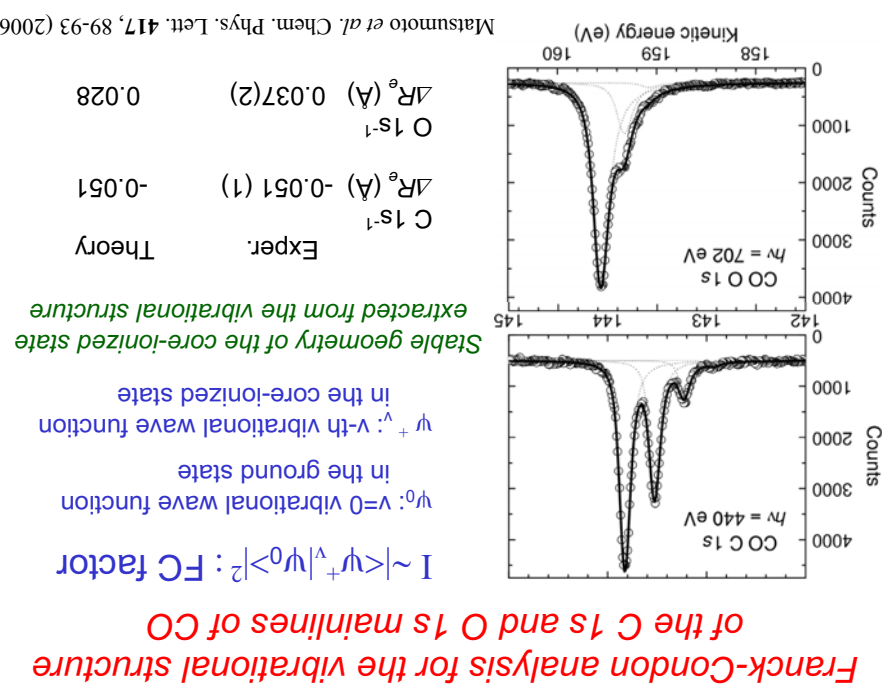
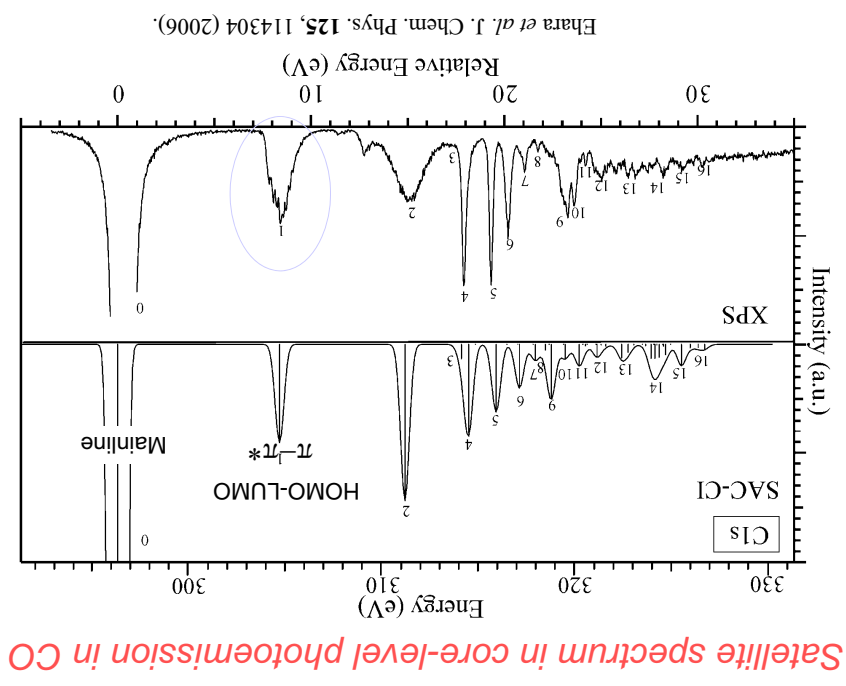
Resonant Auger spectra of Ne "between"

$$\frac{d\theta}{d\sigma} = \frac{4\pi}{\sigma} [1 + \beta P^2(\cos \theta)] \quad \sigma \propto I(0) + 2 \times I(90)$$



Sendai City

Structure of Load Date



H.D. Cohen and U. Fano, Phys. Rev. **150**, 30 (1966).

Interference oscillatory structure becomes much smaller but remains!

$$\Omega_{g,u}(\omega) = \Omega_0(\omega) [1 \pm XCF(k)], \quad XCF(k) = \frac{\sin kR}{kR}$$

Orientational average: Cohen-Fano formula

$$R = R_1 - R_2.$$

where k : photoelectron momentum; R_1, R_2 : position vectors of N(1) and N(2)

Two center photoelectron wave interference fringe

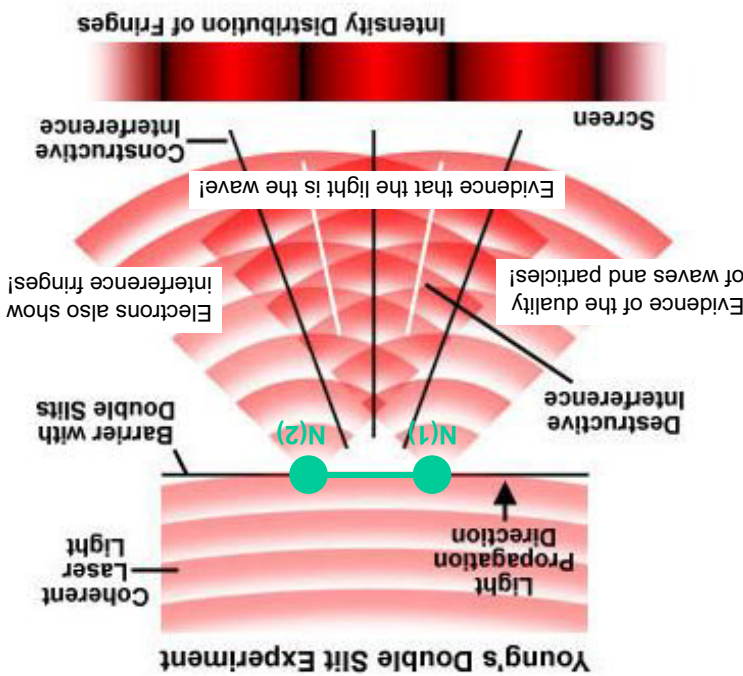
$$\Omega_{g,u}(\omega) \propto \frac{1}{2} |e^{ik \cdot R_1} \mp e^{ik \cdot R_2}|^2 = 1 \mp \cos(k \cdot R),$$

Core-level photoemission from fixed-in-space N^2 :

$$\text{Molecular core-level orbitals: } 1\Omega_{g,u} = \frac{1s_1 \mp 1s_2}{\sqrt{2}}.$$

Two 1s orbitals in N^2 correspond to Young's double slits.

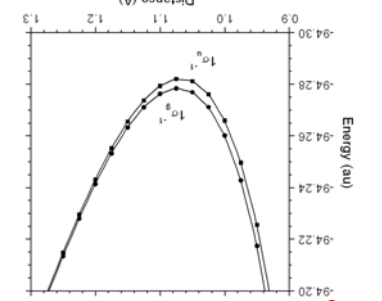
Cohen-Fano two-centre interference



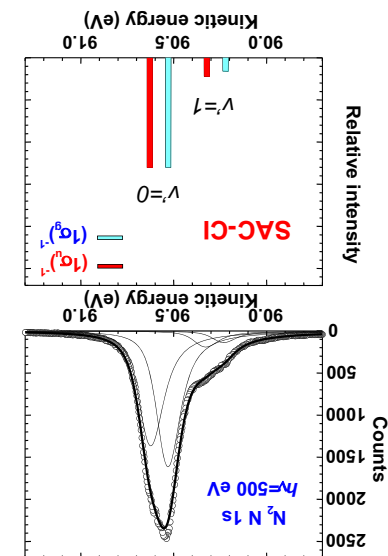
Ehara et al., JCP **124**, 124311 (2006)

$\Delta R_g(A)$	-0.018(1)	-0.017
$\Delta R_u(A)$	-0.023(1)	-0.021
Theory		

Equilibrium geometries extracted from the core-ionized states extracted from the vibrational structure

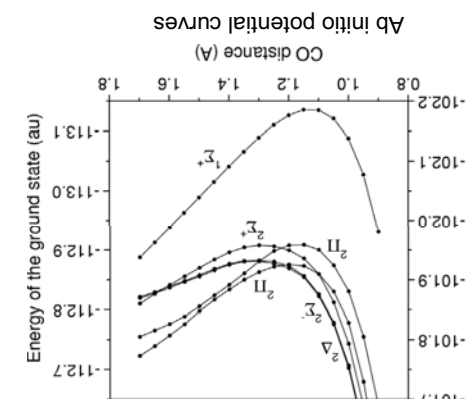


Frank-Condon analysis for the vibrational structure of the $N 1s 1\Omega_g$ and $1\Omega_g$ mainlines of N^2

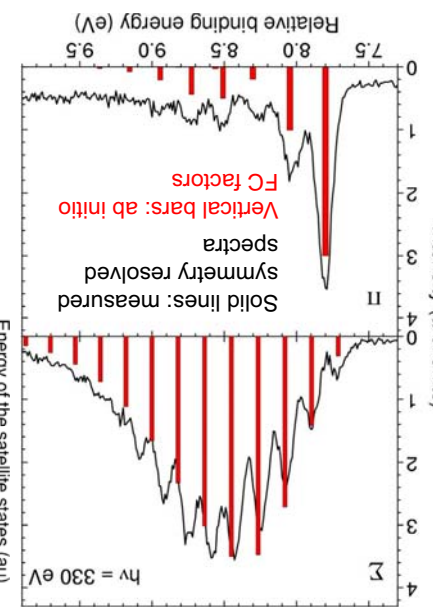


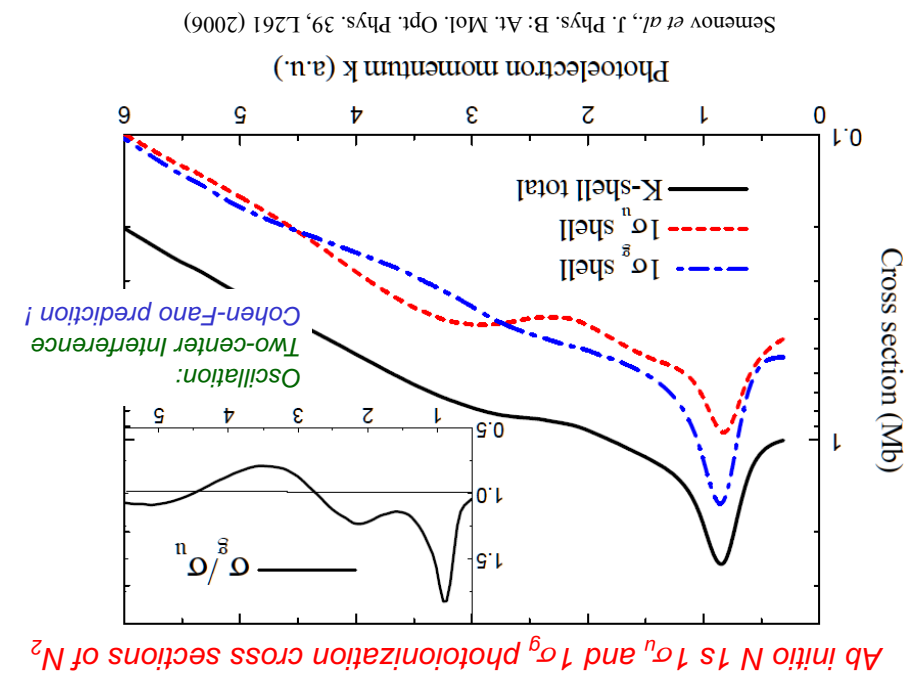
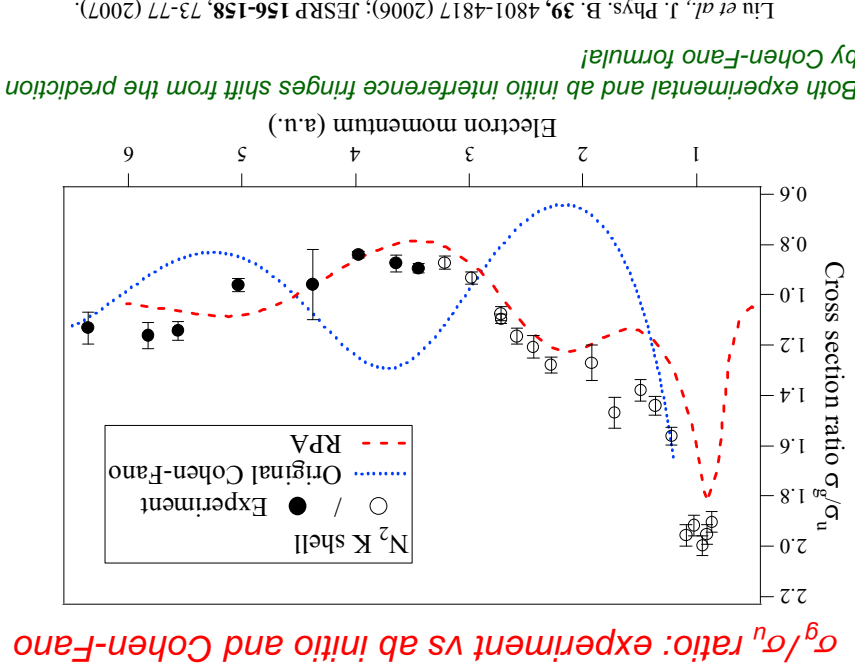
Ueda et al., Phys. Lett. **94**, 243004 (2005).

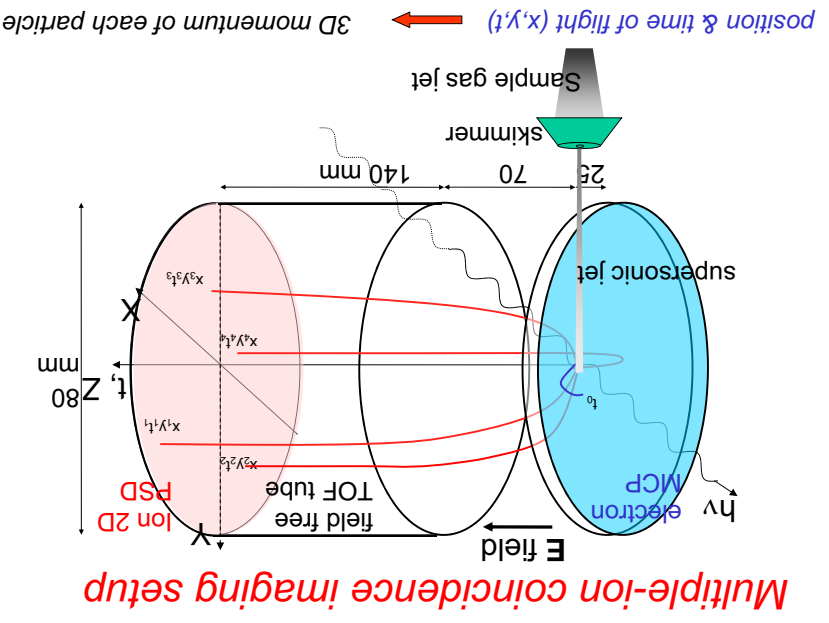
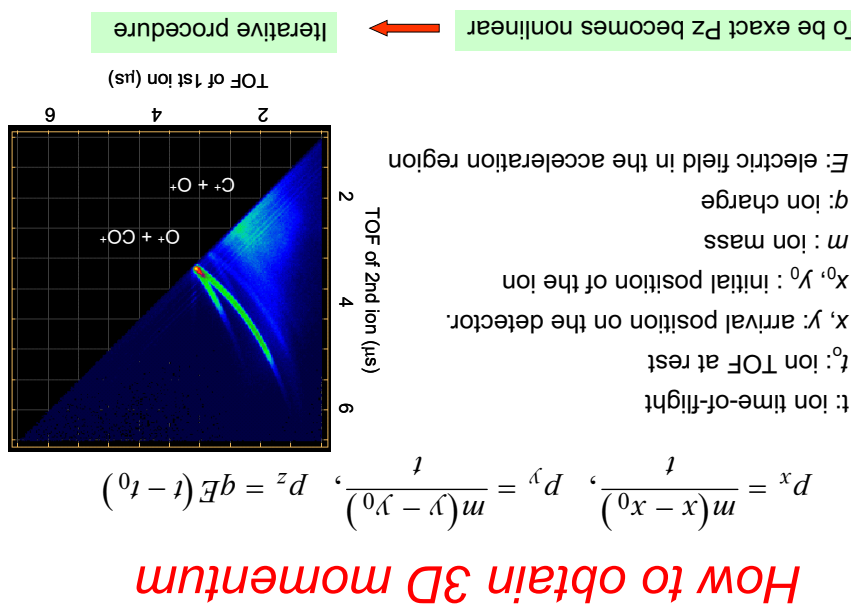
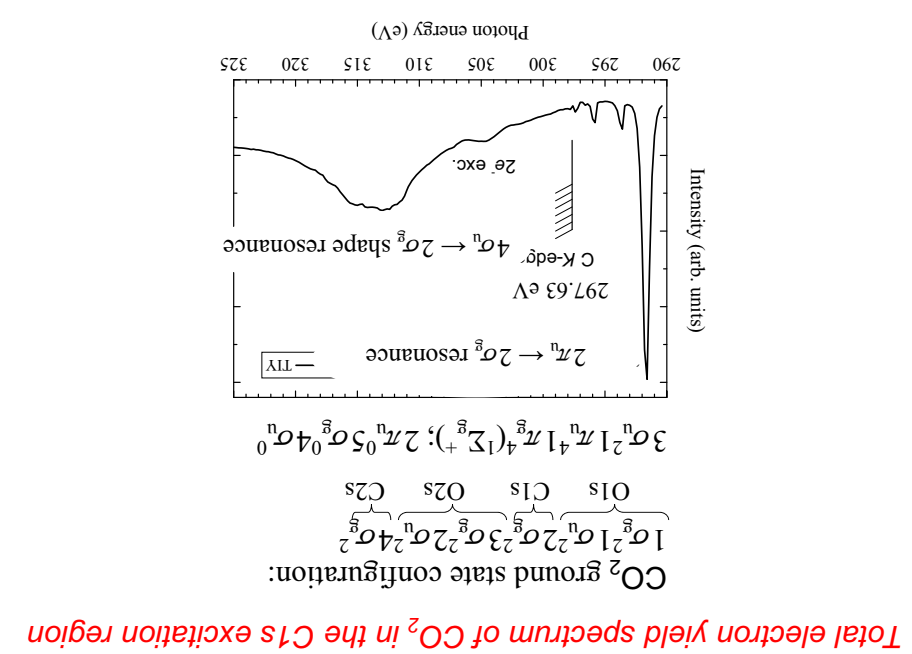
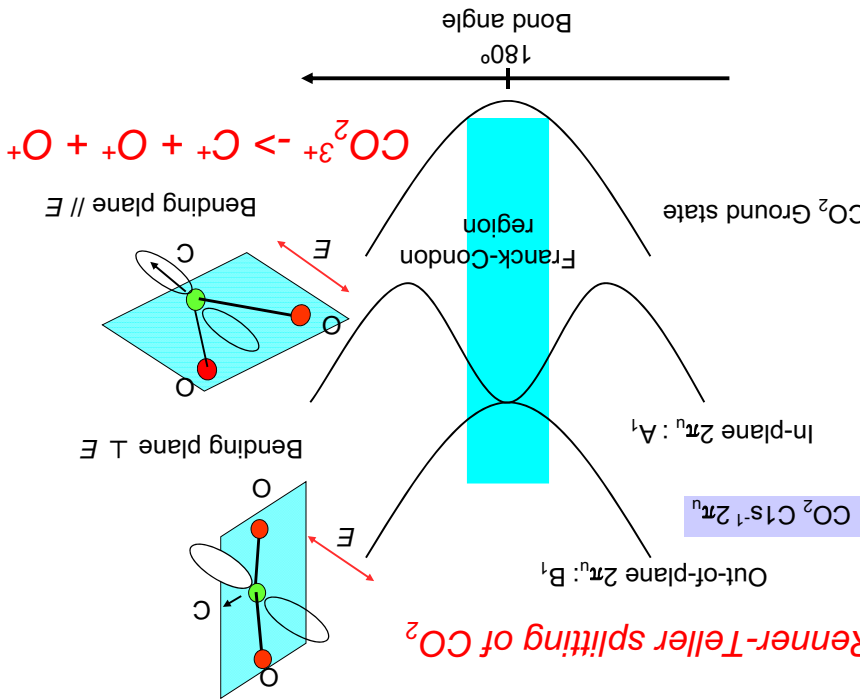
Ab initio FC factors reproduce the measured vibrational distributions.



Frank-Condon analysis of the vibrational structure in the symmetry-resolved C 1s satellite bands of CO

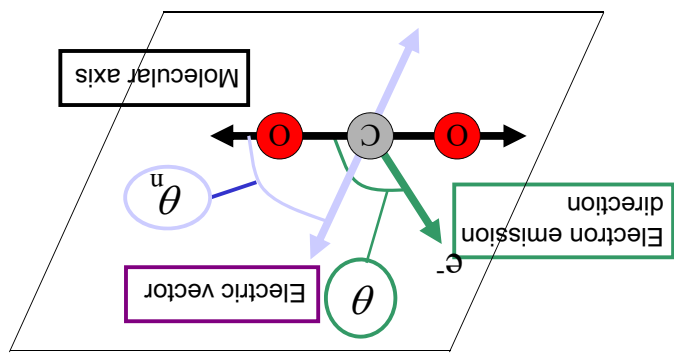






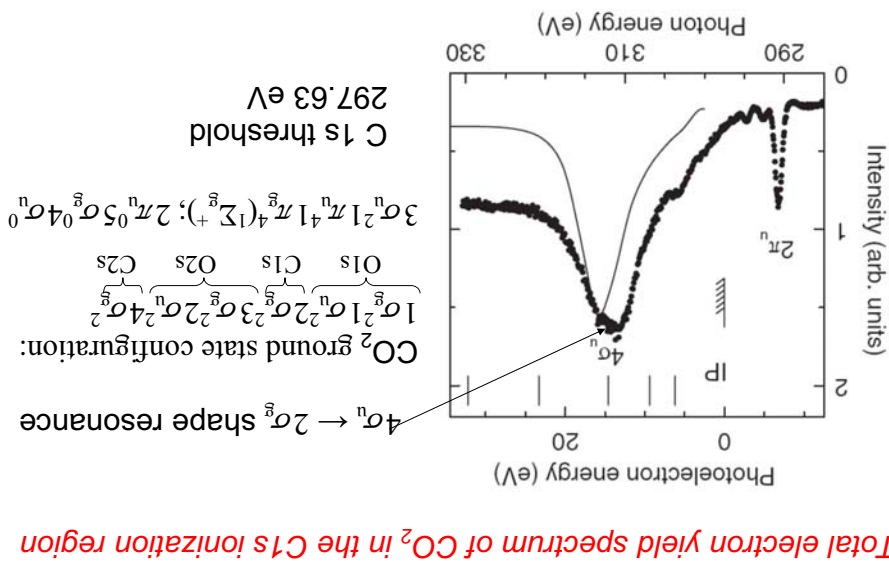
We focus on the electron emission within this reaction plane

N. Saito et al., J. Phys. B, 36 L25 (2003).



Reaction plane = plane define by the E vector and molecular axis

Reaction plane

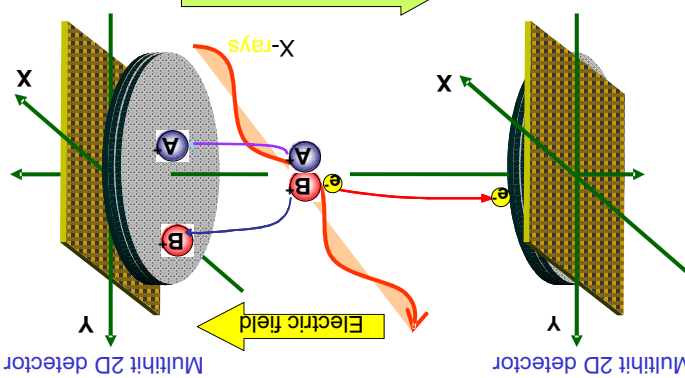


Total electron yield spectrum of CO_2 in the $\text{C}1s$ ionization region

Towards photoelectron diffraction measurement

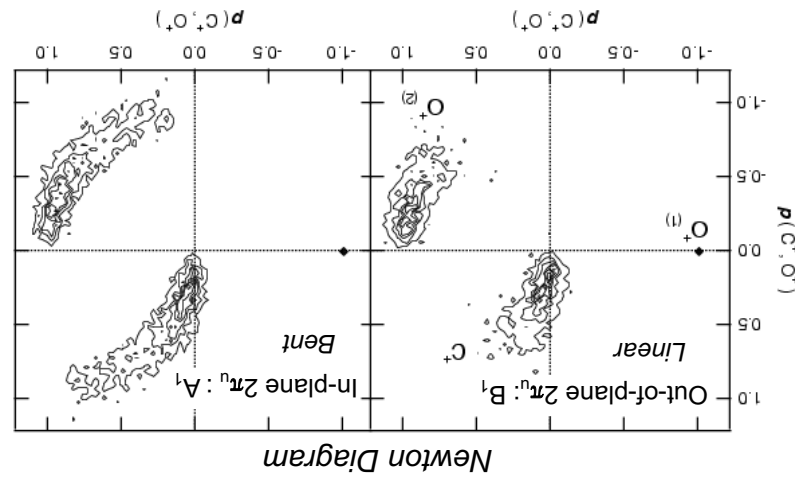
Muramatsu et al., Phys. Rev. Lett. 88, 133002 (2002).

Electron-ion coincidence
Ion momentum conservation
Retrieval of the source point
Molecular frame
Angular distribution



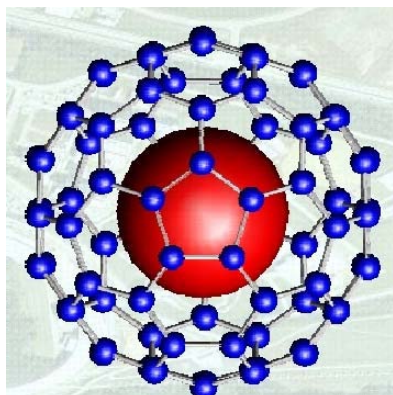
Electron-ion coincidence momentum imaging

Snapshot of the bending motion in the core-excited state with a lifetime ~ 7 fs



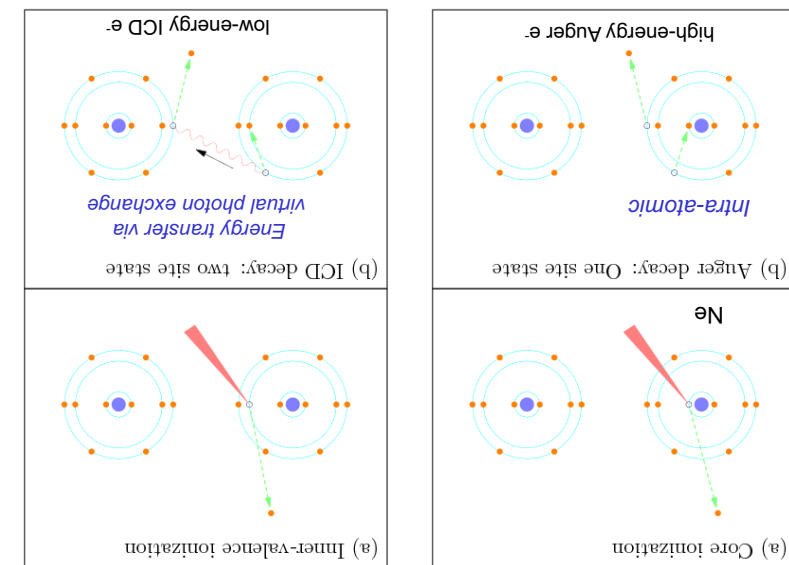
Why is ICD important?

ICD: electronic decay where the environment plays a role!
 ICD takes place in van der Waals clusters, in hydrogen bonding clusters, in metallofullerenes, in bio-molecules in the living cell, etc
 ICD is one of the key players in energy and charge transfer in these systems

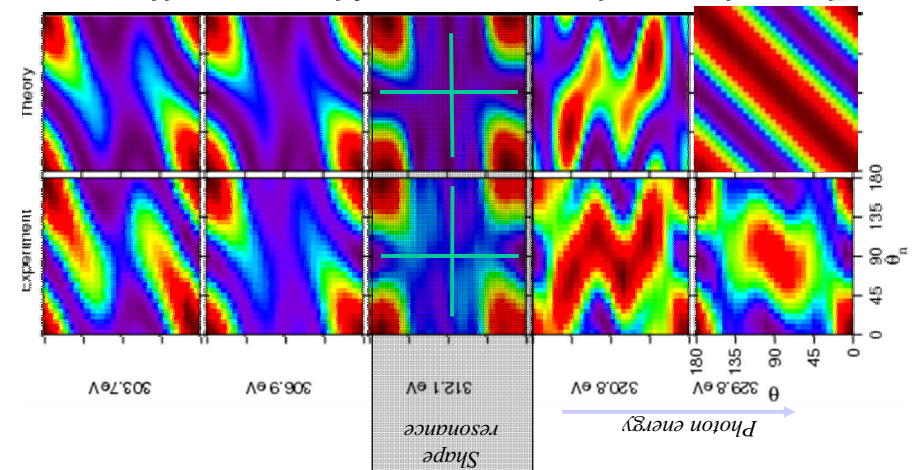


Metal atom in C₆₀

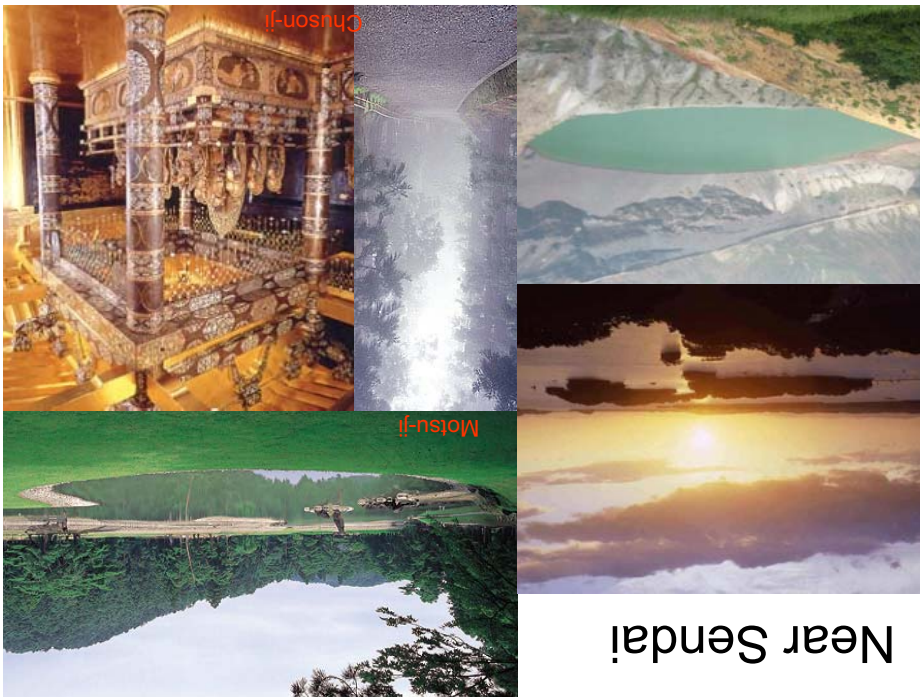
Auger vs Interatomic Coulombic Decay (ICD)

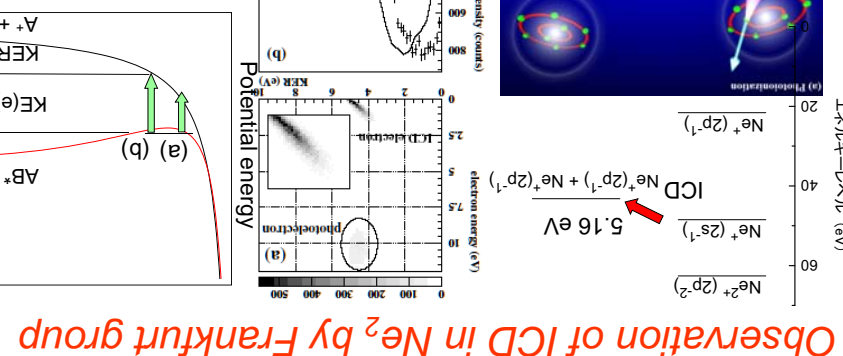


The general agreement between experiment and theory is reasonable. At the shape resonance, the intensity drops at $\theta = 90^\circ$, i.e., ω_{\parallel} photolelectron wave is transmission. The intensity drops at $\theta = -90^\circ$, i.e., ω_{\perp} parallel transition.



C1s photoelectron diffraction (MFAD) of CO₂:





Theoretical Coulombic Decay (ICD)

First observation - Ne cluster:

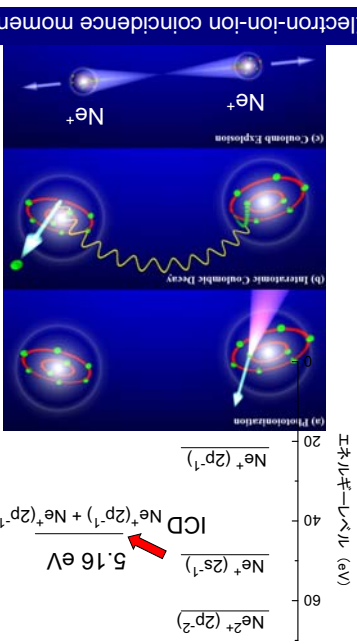
U. Hergenhahn and coworkers, Phys. Rev. Lett. 90, 203401 (2003).

Cluster-size-dependent lifetime:

G. Ohwari et al., Phys. Rev. Lett. 93, 173401 (2004).

Ne_2 -e-ion-ion coincidence:

R. Dörmer and coworkers, Phys. Rev. Lett. 93, 163401 (2004).



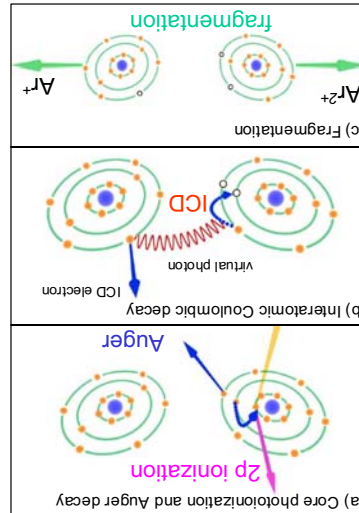
Interatomic Coulombic Decay (ICD)

Experimental evidence of interatomic Coulombic decay from the Auger final states in argon dimers



Using e-e-i coincidence momentum spectroscopy
We detect ICD electrons in coincidence with Ar^+ and Ar^{2+}

Moritschta et al. Phys. Rev. Lett. 96, 243402 (2006).



Labeling electron emission site via the ionic charge state

ICD is one of the important mechanisms to produce low energy electrons after Auger decay!

Radiation damage caused by low energy electron collisions, not high energy Auger electrons.

Radiation damage, caused by e.g., X-ray radiation, is initiated by core ionization.

Radiation damage caused in bio-molecules in the living cell

Why is ICD after Auger decay interesting and important?

R. Samhia and L.S. Cederbaum, Phys. Rev. Lett. 90, 153401 (2003).

Prediction - ICD from Auger final states in Ne dimer:

R. Samhia and L.S. Cederbaum, Phys. Rev. Lett. 90, 153401 (2003).

Interatomic Coulombic Decay after Auger decay

We can experimentally answer to this very basic question?

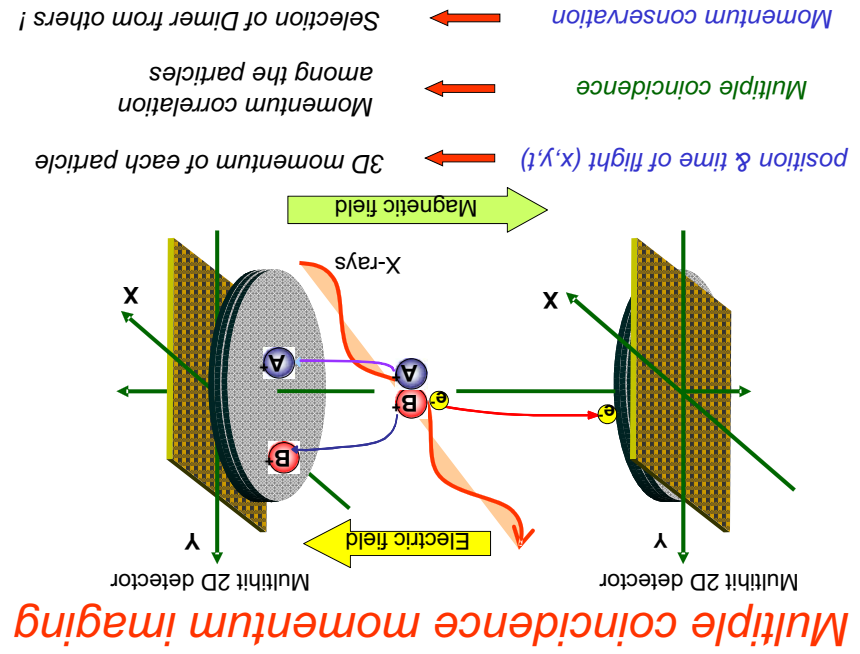
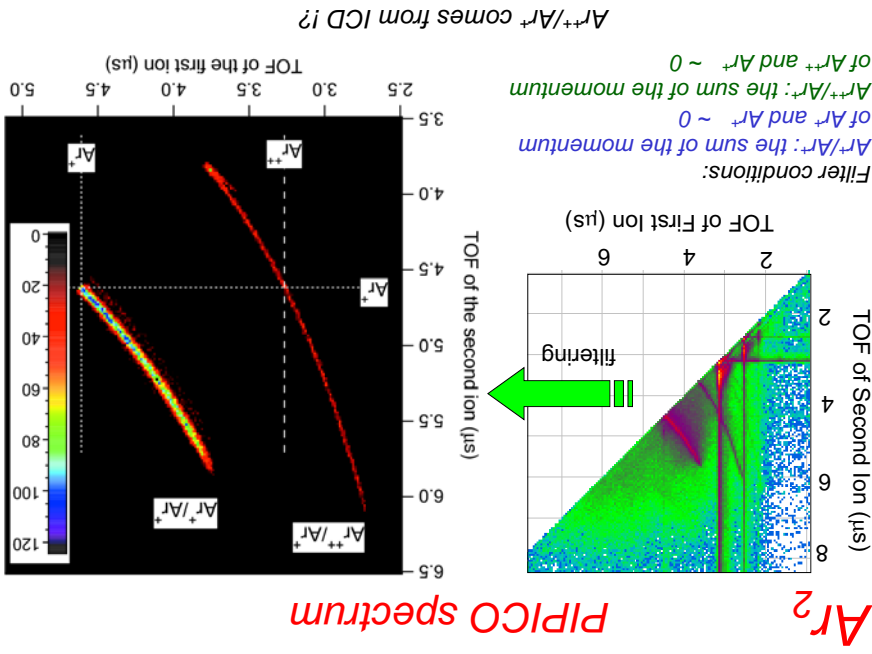
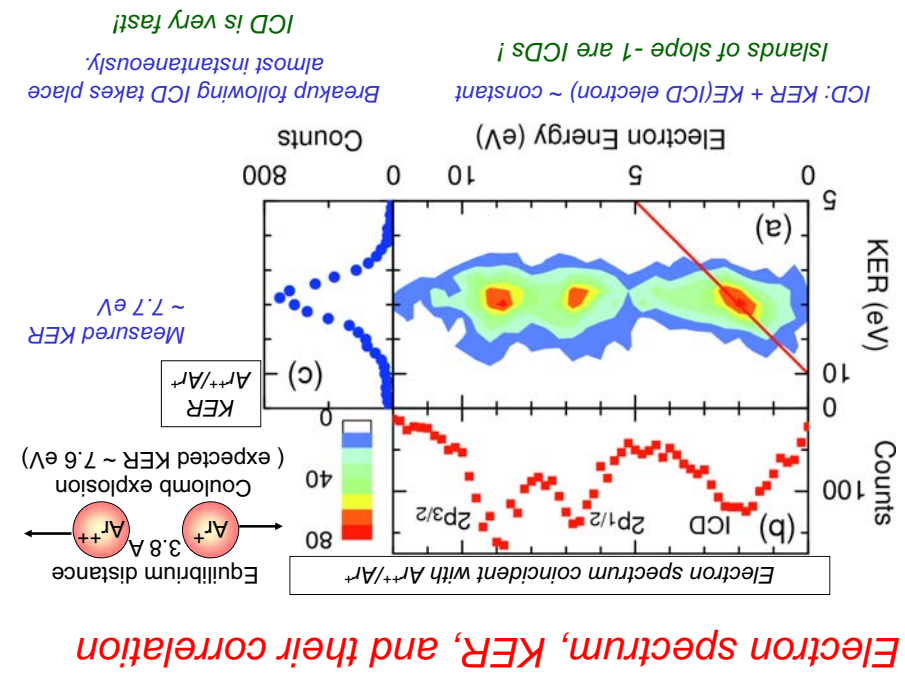
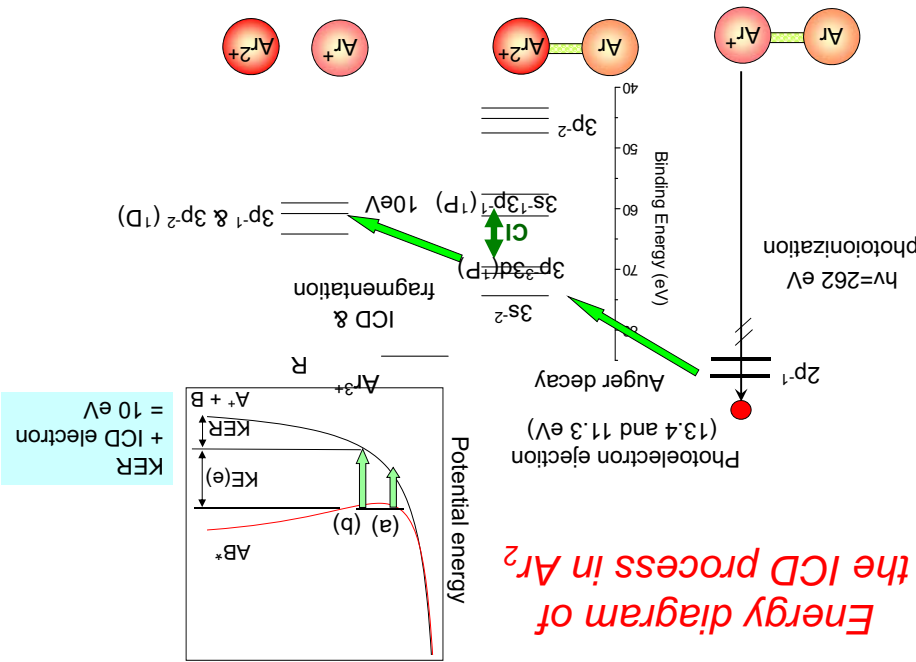
Can the A^+ or Ar^{2+} be which-way information of the double slit experiment?

Is the ICD electron ejected from the A^+ site or Ar^{2+} ?

$[\text{A}^+ (\text{core}-\text{I}) - \text{A}^+] + e_{\text{photo}} \rightarrow [\text{A}^{2+} - \text{A}^+] + e_{\text{Auger}} \rightarrow [\text{A}^{2+} + \text{A}^+] + e_{\text{ICD}}$

ICD is one of the important mechanisms to produce low energy electrons after Auger decay!

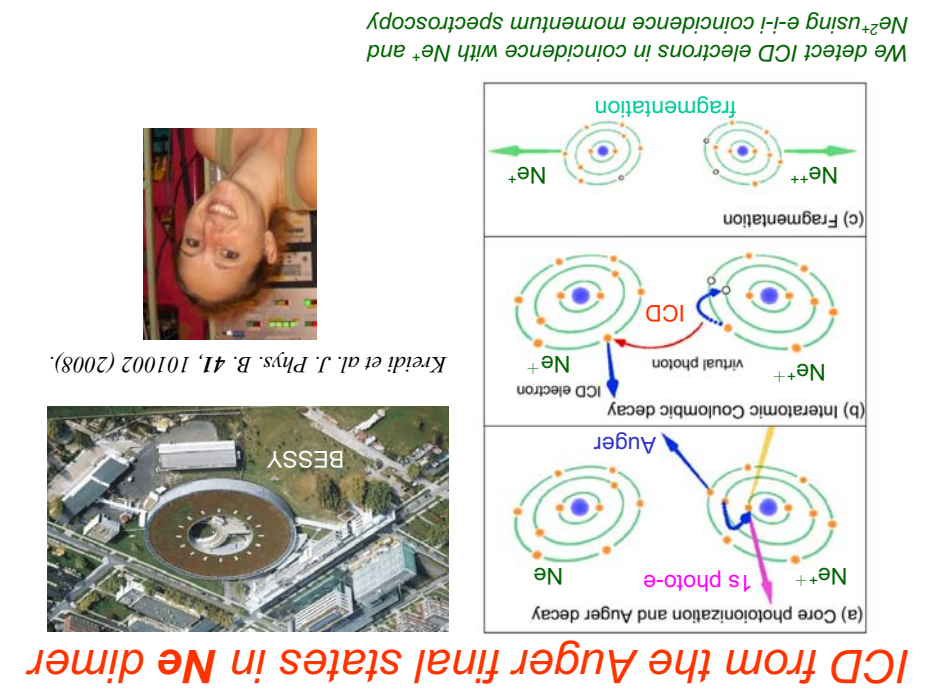
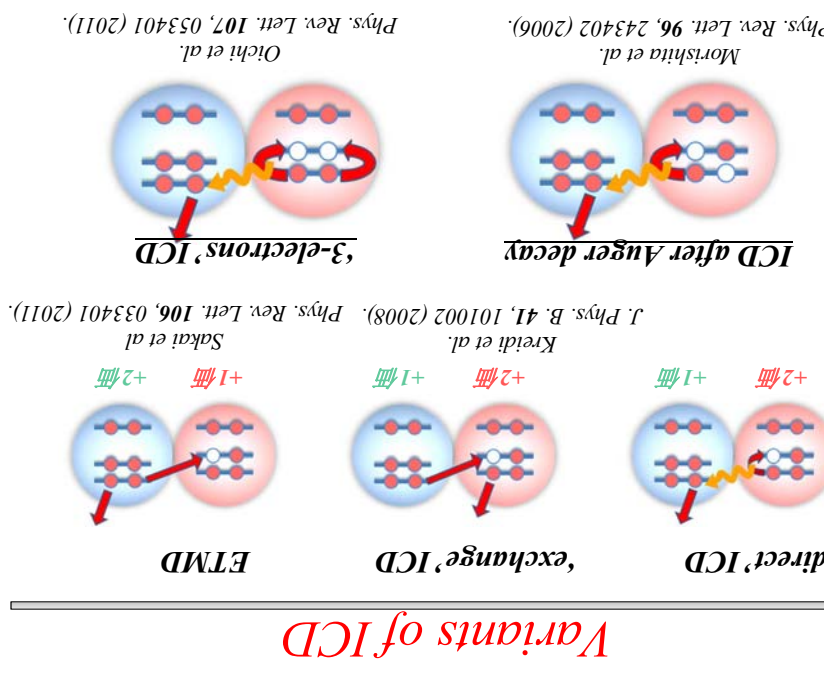
Radiation damage is known to be caused by low energy electron collisions, not high energy Auger electrons.





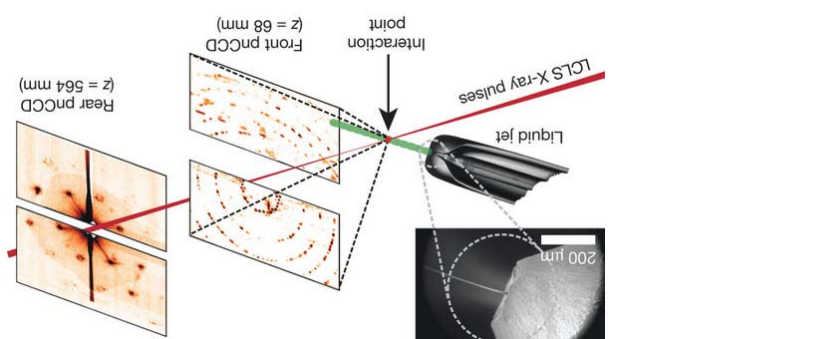
Swiss FEL (2016), Korean FEL,
Shanghai FEL, etc., are coming!

EUV-X FELs in the World

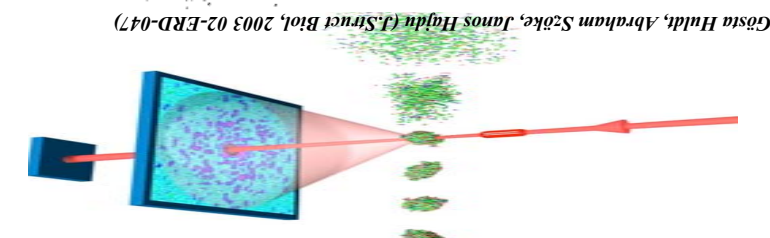


Characteristic properties of FEL pulses

Intense and ultra-short pulses at X-rays
Why X-rays? structure determination at atomic resolution
Femtosecond X-ray Protein Nanocrystallography; Chapman et al., *Nature* 470, 73–77 (2011).

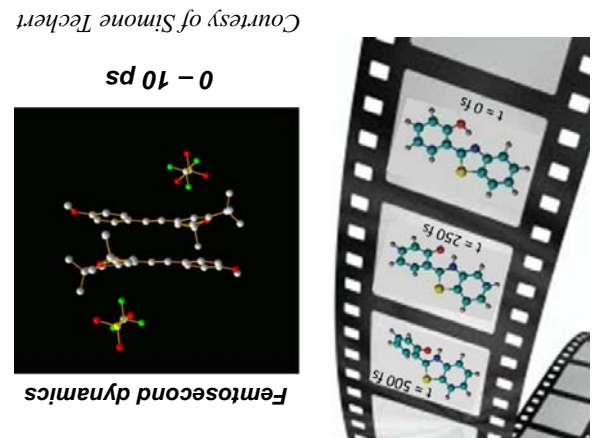


Cohherent X-ray imaging of non-crySTALLized samples
at short wavelengths (EUV to X-rays)



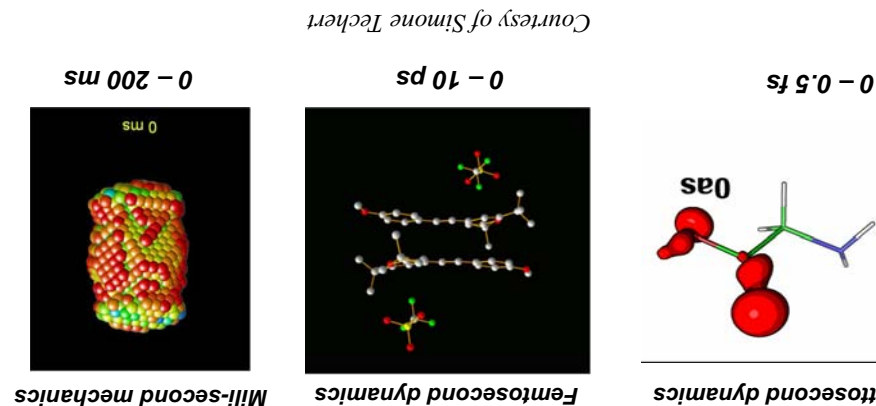
Characteristic properties of FEL pulses

ultra-short ($100 - 10 \text{ fs}$)



Characteristic properties of FEL pulses

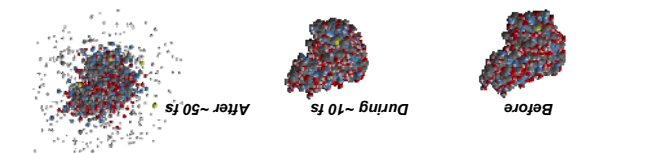
ultra-short ($100 - 10 \text{ fs}$)



High-Resolution Protein Structure Determination by Serial Femtosecond Crystallography; Boure et al. *Science* 337 (6092) 362 (2012).

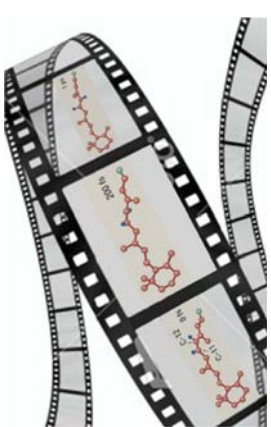
Single Mimivirus Particles Intercepted and Imaged with an X-ray laser
Seibert et al. *Nature* 470, 78–81 (2011)

Neutze, Wouts, van der Spoel, Weckert, Hajdu *Nature* 406, 752 (2000)



Characteristic properties of FEL pulses

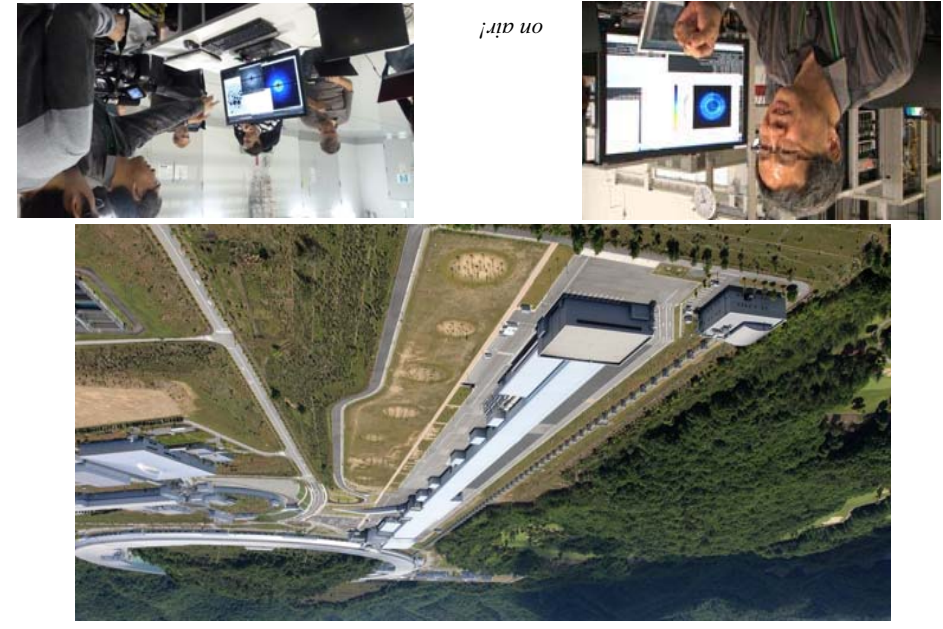
Catching atomic motion in reaction
(molecular movie)



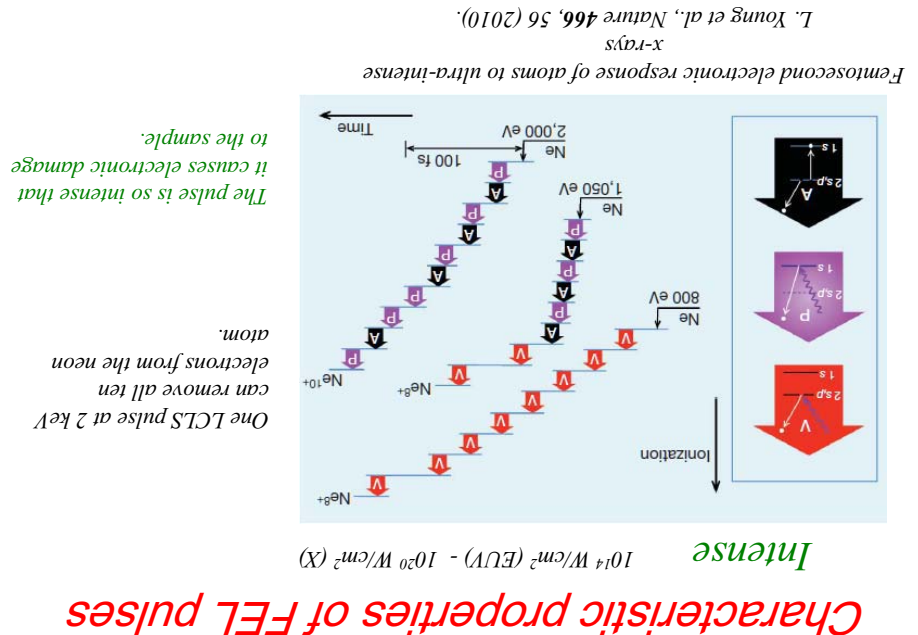


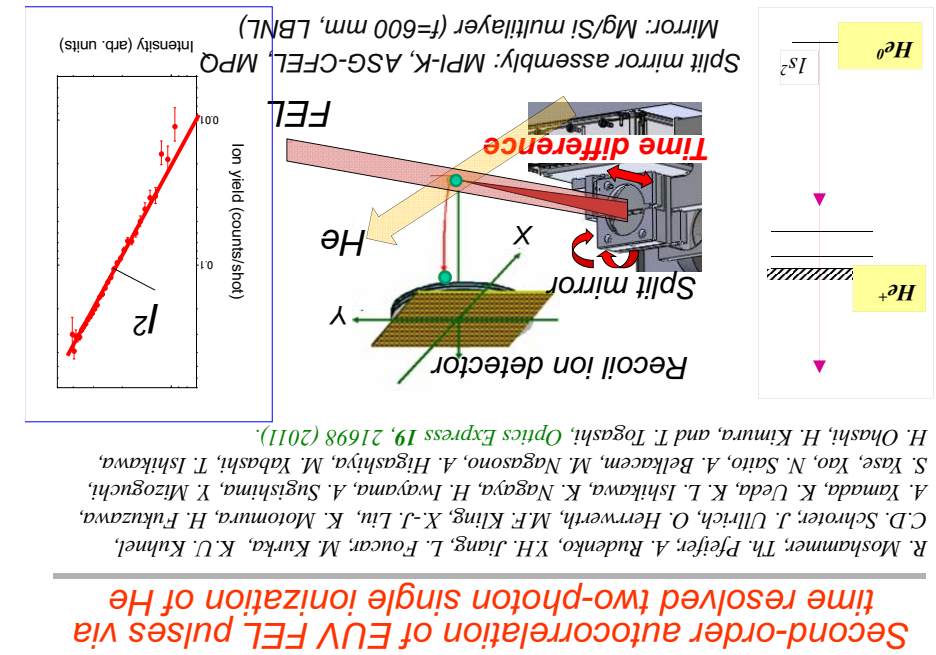
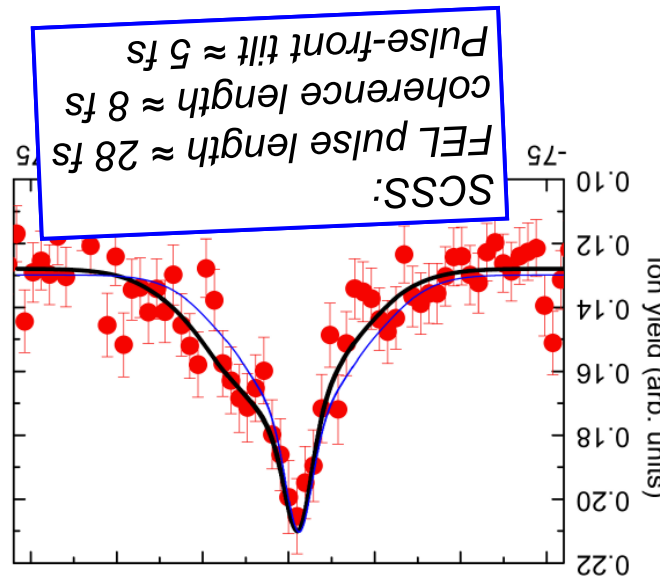
SACLA XFEEL

- **Short wave-length: toward Hard X-rays**
- **Structure determination at atomic resolution**
- **Cohere nt**
- **Coherent X-ray imaging of non-crystallized samples**
- **Ultrafast** $100\text{-}10\text{ fs}$: resolving atomic motion $\rightarrow \sim 200\text{ as}$: resolving electron wave-packet motion
- **Intense** 10^{14} W/cm^2 (EUV) - 10^{20} W/cm^2 (X)
- **Ligh t matter interaction** $\text{Non-linear response}$
- **Electr onic damage**
- **Warm (Hot) dense matter science**

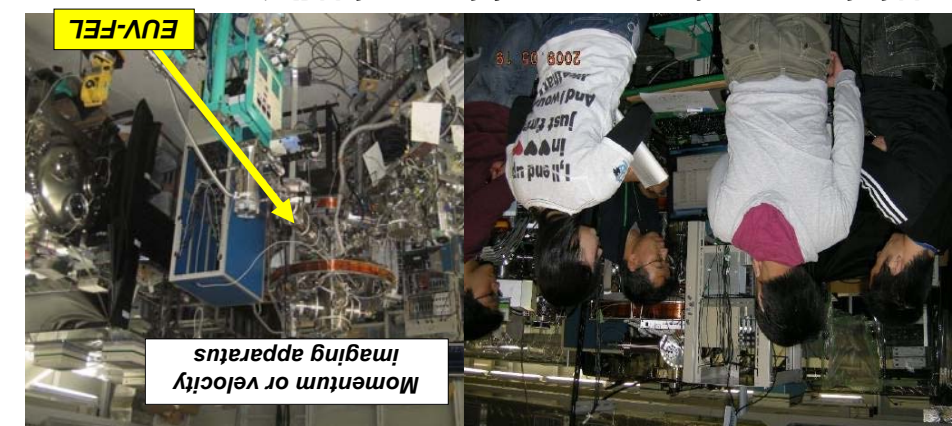


SACLA (XFEL based on 7 June 2011)





- Second-order autocorrelation of SCS EUV-FEL pulses via time-resolved two-photon single ionization of He
- Photoelectron angular distributions for two-photon ionization of He atoms by SCS EUV-FEL pulses
- Potential of coherent control via seeded FEL
- Deep inner-shell multi-photon absorption of Ar and Xe atoms by SACLA XFEL pulses
- Relevance to the electronic radiation damage

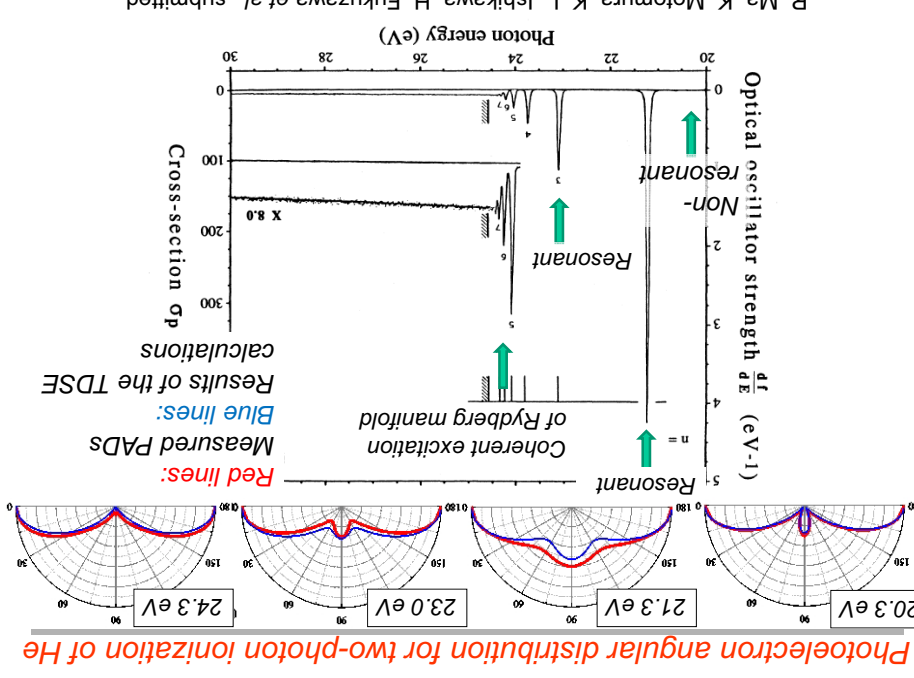


SCS test accelerator : EUV-FEL (20-24 eV)

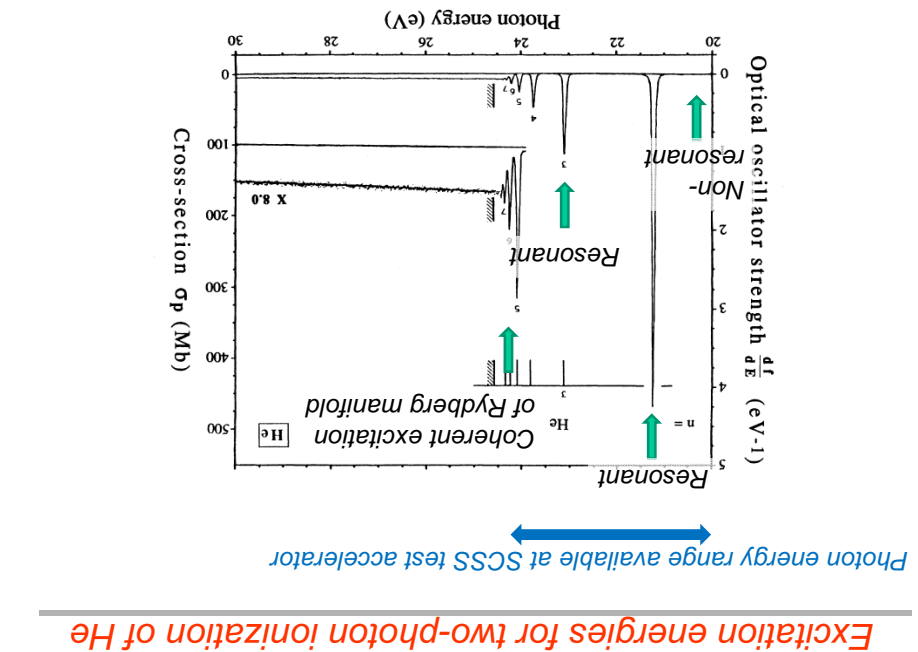
Multipole ionization of rare gas atoms and clusters: with M. Yao's group
VMI: with help of M. Vrakking's group
Autocorrelation: with J. Ullrich's group

Experimental evidence for competition between the resonant and non-resonant two-photon ionization

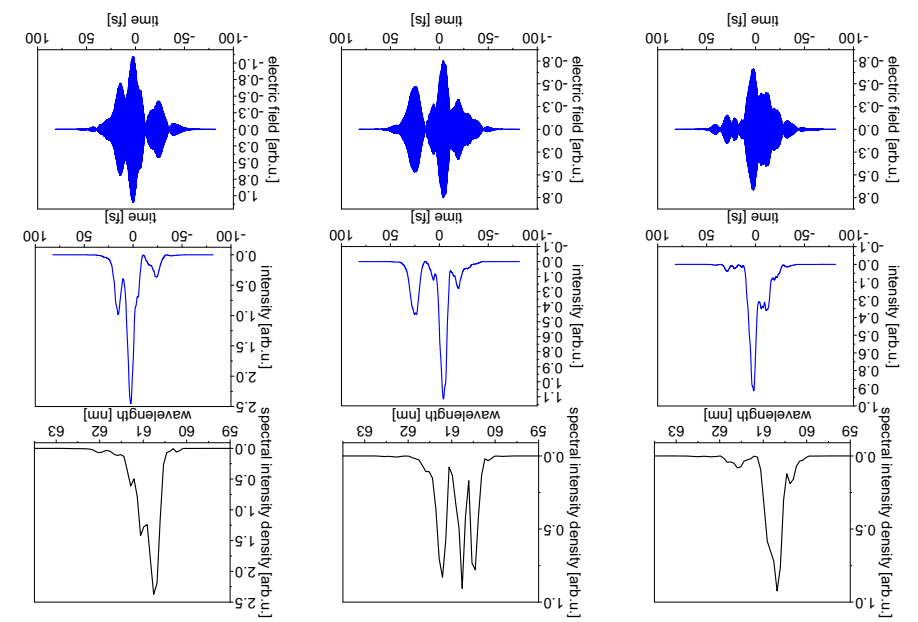
Y. Ueda, K. Nagaya, S. Yase, Y. Mizoguchi, M. Yao, A. Rousee,
M. Hundermarck, M. Vrakking, P. Johnsson, M. Nagasano, K. Tono,
T. Ogashi, Y. Senba, H. Ohashi, M. Yabashi, and T. Ishikawa

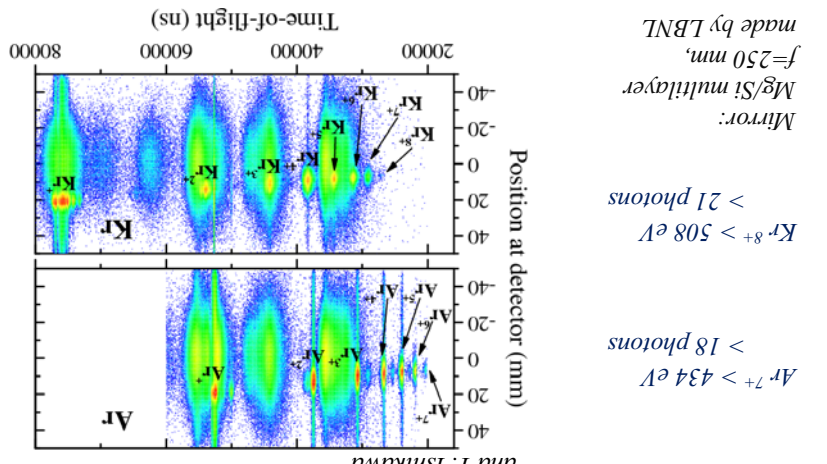


W. F. Chan et al., Phys. Rev. A 44, 186 (1991).



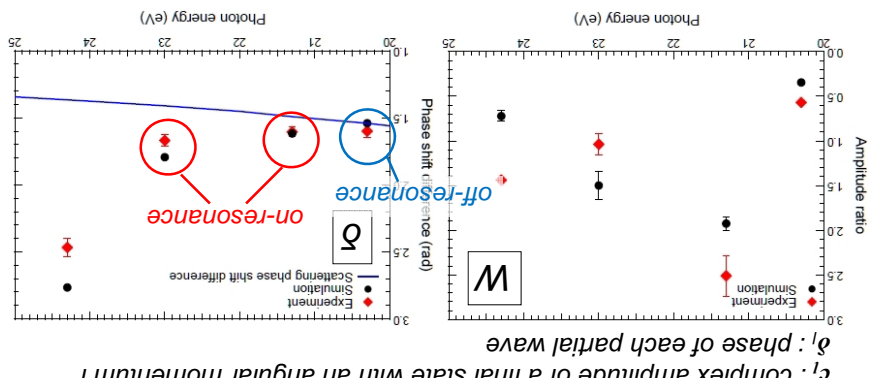
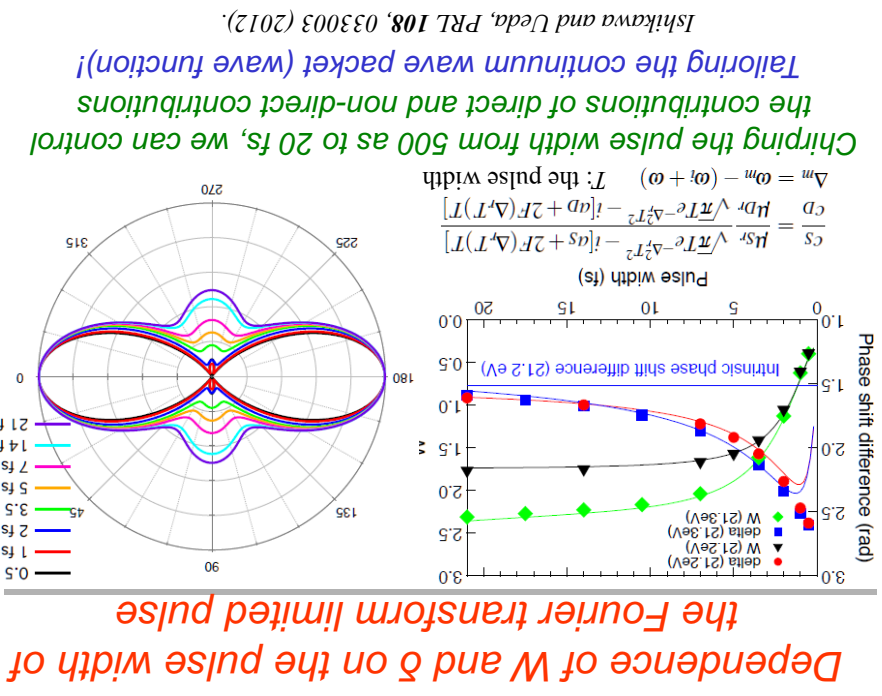
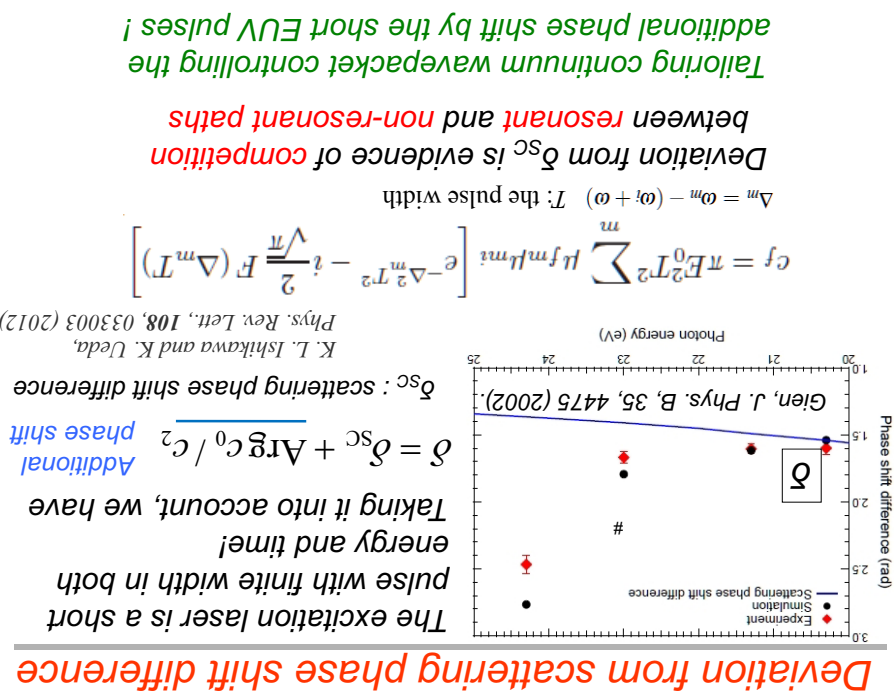
CSS Sample Pulse Shapes



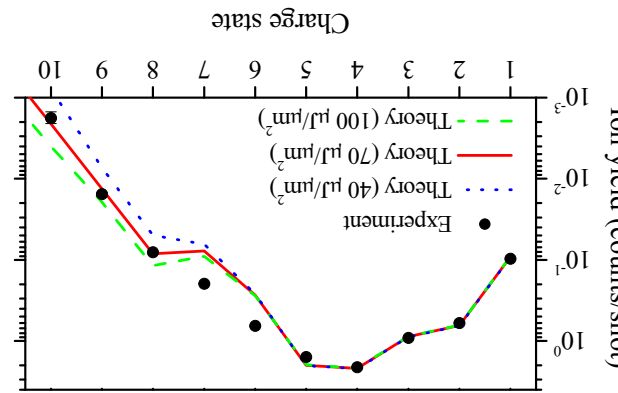


M. Nagasano, A. Higashiyama, T. Togashi, H. Ohishi, and H. Kimura, M. Yabashi, J. Ulich, K. Ueda, N. Saito, H. Murakami, M. Yao, A. Bellacemi, R. Fefel, H. Hayama, K. Nagaya, X.-J. Liu, H.-U. Kühnel, G. Pfeiffer, P. Labropoulos, K. Motomura, H. Fukuzawa, K. Papamichael, M. Kurka, A. Rudenko, L. Foucar, and T. Ishikawa

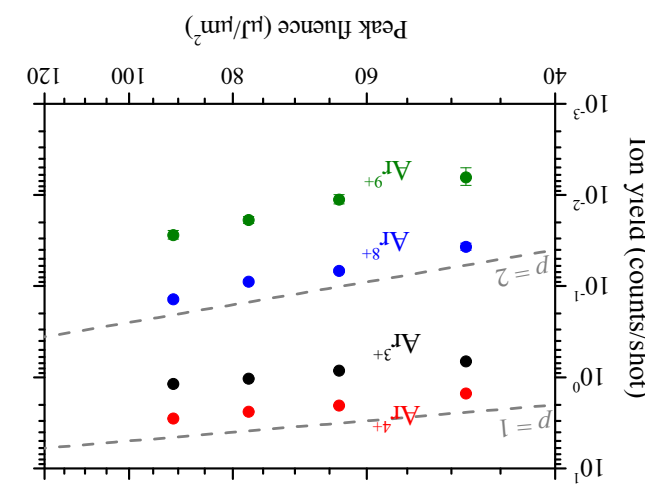
multiple ionization of rare gas atoms irradiated by EUV
free-electron laser pulses at 51 nm



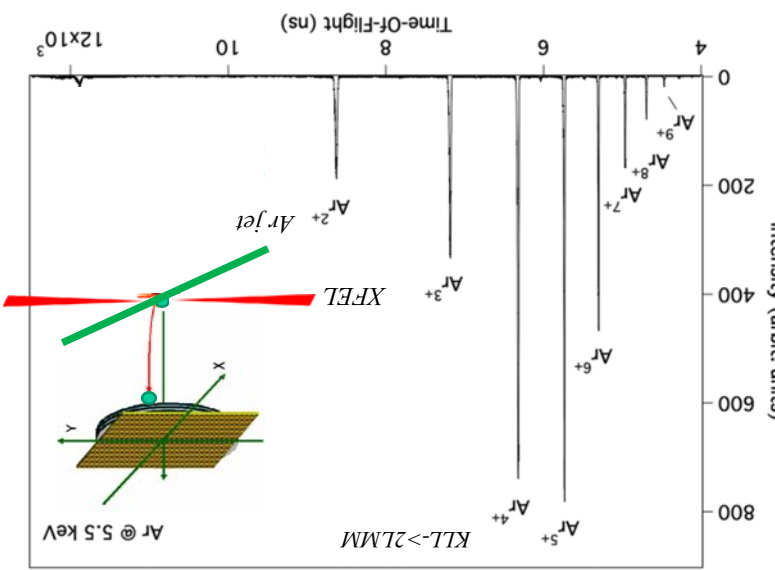
By comparison with theory,
we obtained peak fluence of
 $70 \mu\text{J}/\mu\text{m}^2$ in the experiment.
In the theory, the pulse shape
of Gaussian of 30 fs (FWHM),
and Gaussian focal shape of
 $1 \mu\text{m}$ (FWHM) $\times 1 \mu\text{m}$
(FWHM) are assumed.



Charge state distribution of Arⁿ⁺: experiment and theory



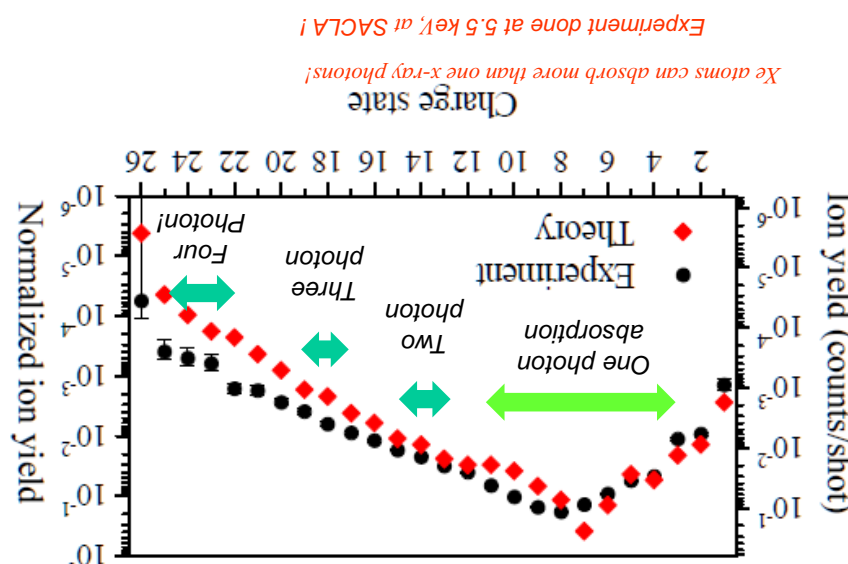
XFEL fluence dependence for Arⁿ⁺ yields



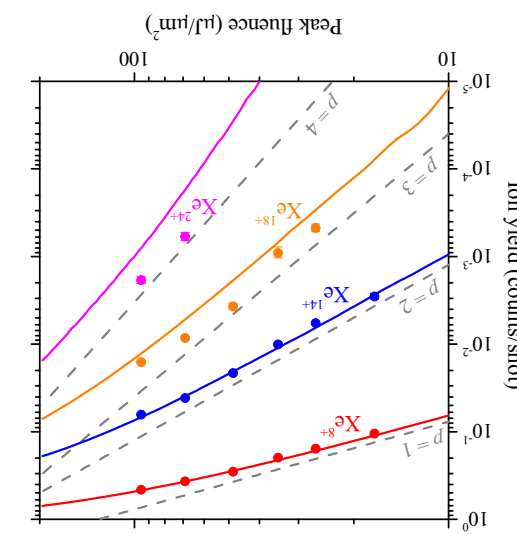
Time-of-Flight spectrum of argon ions



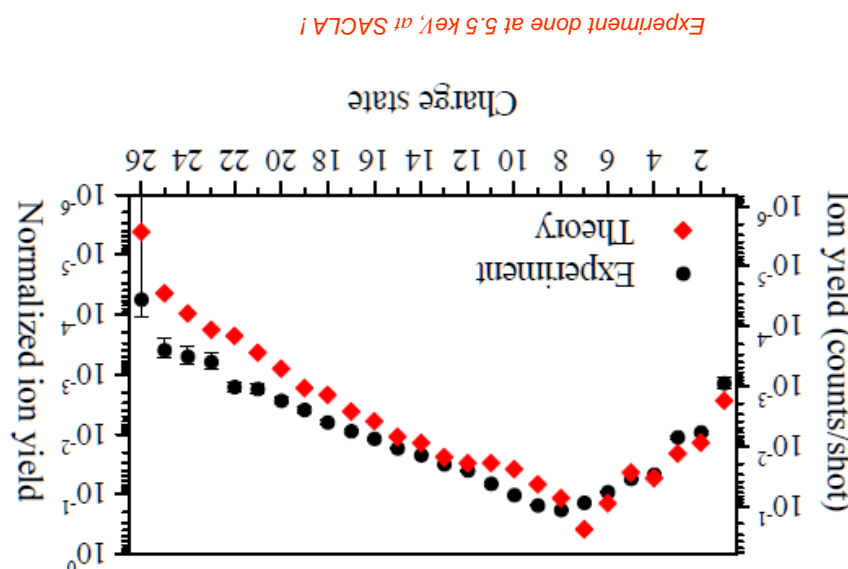
by SACLA XFEL pulses
Deep inner-shell multiphoton absorption of Ar and Xe



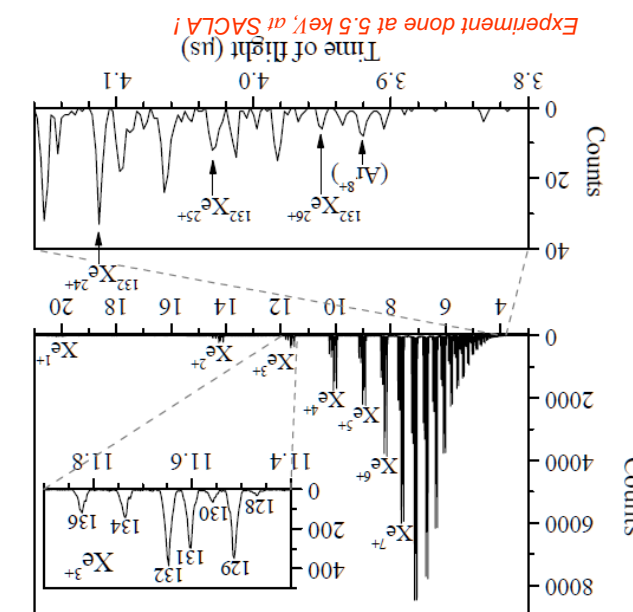
Xenon ion charge distributions (exp: vs theory)



XFEL fluence dependence for Xe^n+ yields



Xenon ion charge distributions (exp: vs theory)

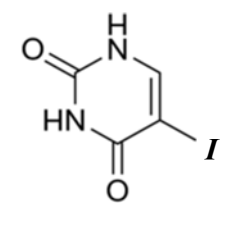
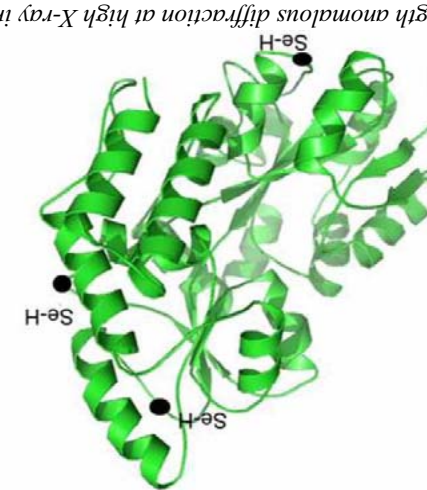


Time of flight spectrum of xenon ions

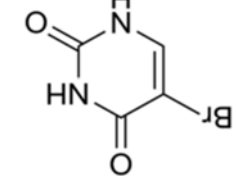
A couple postdoc positions are open at
Tohoku University for SACLAC project!



Reliance to other fields: Radiation damage
Deep inner-shell multiphoton ionization by intense x-ray
free-electron laser pulses
H. Fukuzawa, S.-K. Son, K. Motomura, S. Mondal, K. Nagaya,
S. Wade, X.-J. Liu, R. Feifel, T. Tachibana, Y. Ito, M. Kiumura,
T. Sakai, K. Matsunami, H. Hayashita, J. Kajikawa, P. Jonsson, M. Siano, E. Kukk, B. Rudke, B.
C. Mirion, K. Tono, T. Togashi, Y. Imabushi, T. Sato, T. Kawayama,
T. Hatsuji, T. Kameshima, M. Yabashi, M. Yao, R. Santra,
S.-K. Son, H. N. Chapman, and R. Sautra,
Multidavelength anomalous diffraction at high X-ray intensity
Phys. Rev. Lett. **107**, 218102 (2011).



5Br-Uracil



5Br-sensitizer

Anomalous X-ray scattering